STEM CELLS AND DEVELOPMENT
Volume 22, Number 1, 2013

DOI: 10.1089/scd.2012.0116

Neonatal Desensitization Supports Long-Term Survival and Functional Integration of Human Embryonic Stem Cell-Derived Mesenchymal Stem Cells in Rat Joint Cartilage Without Immunosuppression

Shufang Zhang,[1–3] Yang Zi Jiang,[1,2] Wei Zhang,[1,2] Longkun Chen,[2] Tong Tong,[1,2] Wanlu Liu,[1,2] Qin Mu,[1,2] Hua Liu,[1–3] Junfeng Ji,[1–3] Hong Wei Ouyang,[1–4] and Xiaohui Zou[5]

Immunological response hampers the investigation of human embryonic stem cells (hESCs) or their derivates for tissue regeneration in vivo. Immunosuppression is often used after surgery, but exhibits side effects of significant weight loss and allows only short-term observation. The purpose of this study was to investigate whether neonatal desensitization supports relative long-term survival of hESC-derived mesenchymal stem cells (hESC-MSCs) and promotes cartilage regeneration. hESC-MSCs were injected on the day of birth in rats. Six weeks after neonatal injection, a full-thickness cylindrical cartilage defect was created and transplanted with a hESC-MSC-seeded collagen bilayer scaffold (group d + s + c) or a collagen bilayer scaffold (group d + s). Rats without neonatal injection were transplanted with the hESC-MSC-seeded collagen bilayer scaffold to serve as controls (group s + c). Cartilage regeneration was evaluated by histological analysis, immunohistochemical staining, and biomechanical test. The role of hESC-MSCs in cartilage regeneration was analyzed by CD4 immunostaining, cell death detection, and visualization of human cells in regenerated tissues. hESC-MSCs expressed CD105, CD73, CD90, CD29, and CD44, but not CD45 and CD34, and possessed trilineage differentiation potential. Group d + s + c exhibited greater International Cartilage Repair Society (ICRS) scores than group d + s or group s + c. Abundant collagen type II and improved mechanical properties were detected in group d + s + c. There were less CD4+ inflammatory cell infiltration and cell death at week 1, and hESC-MSCs were found to survive as long as 8 weeks after transplantation in group d + s + c. Our study suggests that neonatal desensitization before transplantation may be an efficient way to develop a powerful tool for preclinical study of human cell-based therapies in animal models.

Introduction

Adult articular cartilage has a limited self-reparative capacity after damage, which has stimulated development of autologous chondrocyte implantation (ACI) for regeneration of articular cartilage. Despite overall improvement of joint function and therapeutic efficacy since its clinical application in 1980s [1], the number of autologous chondrocytes is limited, and they tend to dedifferentiate during in vitro expansion [2]. Moreover, transplanted autologous chondrocytes preferentially formed fibrocartilage tissue instead of hyaline cartilage in the defects [3]. These limit future application of ACI and warrant further exploration of new cell sources such as stem cells for cartilage repair.

Embryonic stem cells (ESCs) are able to differentiate into various cell types, including chondrocytes in vitro, and thus are considered as one of the cell sources for tissue regeneration, including cartilage tissue. Previous studies have reported that implantation of ESCs or ESC-derived chondrogenic cells promoted cartilage repair in vivo [4–6]. However, it is difficult to obtain autologous ESCs for cell transplantation, and an immunologic barrier prevents in vivo long-term engraftment and function of allogenous ESCs [7]. Immunosuppressants are usually used to overcome the immune response. However, they cause severe side effects and make animals difficult to survive during this period. Without immunosuppression, human ESCs (hESCs) were rejected after 7 days of transplantation into immunocompetent animals

[1]Center for Stem Cell and Tissue Engineering, School of Medicine, Zhejiang University, Hangzhou, Zhejiang, China.
[2]Zhejiang Provincial Key Laboratory of Tissue Engineering and Regenerative Medicine, Zhejiang University, Hangzhou, Zhejiang, China.
[3]Department of Stem Cell and Regenerative Medicine, School of Medicine, Zhejiang University, Hangzhou, Zhejiang, China.
[4]Soft Matter Research Center, Zhejiang University, Hangzhou, Zhejiang, China
[5]Clinical Research Center, The First Affiliated Hospital, School of Medicine, Zhejiang University, Hangzhou, Zhejiang, China.

such as mice [8]. A long-term effect of hESC-derivates transplantation on *in situ* cartilage regeneration was only observed in immunodeficient animal models such as nude mice [9]. However, the long-term effect of hESCs on joint cartilage regeneration in an appropriate immunocompetent animal model remains unknown. It was reported that neonatal injection can induce immune tolerance and allow long-term immune protection of xenoplants in host rats [10], thus enabling proper preclinical assessment of functional efficacy of human cells for central nervous system disease therapy.

In this study, we utilized this neonatal desensitization to achieve long-term survival of hESC-derived mesenchymal stem cells (hESC-MSCs) after implantation without immunosuppression for rat cartilage tissue regeneration. Neonatal desensitization alleviated immune response as shown by reduced inflammatory cell infiltration, supported the long-term survival of transplanted hESCs-MSCs, and therefore led to the improvement of cartilage regeneration.

Materials and Methods

Bilayer collagen scaffold fabrication

The bilayer collagen scaffold was fabricated according to our previous study [11]. Briefly, insoluble type I collagen was isolated and purified from pig Achilles tendon and dissolved in 0.5 M acetic acid (1.0 wt%) [12]. The collagen solution was frozen at −80°C, lyophilized in a freeze dryer (Heto Power Dry LL1500), and compressed mechanically. The new collagen solution was added onto the compressed collagen matrix and freeze-dried again to make a second layer. The scaffold was crosslinked by severe dehydration (dehydrothermal crosslinking) [13] and made as a cylinder 2 mm in diameter and 2 mm in height before use.

Cell culture

hESC-MSCs were derived from an undifferentiated NIH-registered hESC H9 cell line as previously described [14]. Briefly, a confluent 6-well plate of hESCs was trypsinized for 5 min at 37°C, centrifuged, resuspended in a knockout Dulbecco's modified Eagle's medium (DMEM; Gibco) [15], supplemented with 10% serum replacement medium (Gibco) and 5 ng/mL fibroblast growth factor (FGF) 2 (Gibco), and plated on a gelatinized 10-cm plate. The confluent cells were passaged and seeded at the density of 10^2–10^3 cells/cm^2. Cells were cultured in the DMEM supplemented with penicillin–streptomycin and 20% fetal bovine serum (Invitrogen). Most of the cells in the culture appeared fibroblast-like after 2 passages, and then, the cells were seeded at very low density (10 cells/cm^2) to form colonies. The hESC-derived colonies forming fibroblast-like cells were designated as hESC-MSCs. hESC-MSCs at passages 10–15 were used in this study.

Fluorescence-activated cell sorter analysis

Monolayer cultured cells were detached by mechanical scratch and filtered through a stainless steel mesh filter to eliminate cell aggregates from the single-cell suspension. After centrifugation, cells were blocked with 1% bovine serum albumin for 15 min. Then, cells were incubated with 1 μg of phycoerythrin-conjugated mouse anti-human CD44, CD45, CD105, or fluorescein isothiocyanate (FITC)-conjugated mouse anti-human CD34, CD73, CD90 for 1 h at room temperature. Nonconjugated mouse antibodies specific to human CD29 were incubated with cells for 1 h at room temperature. After washing, cells were incubated with rabbit anti-mouse IgG-FITC- conjugated second antibody for 30 min on ice. After fixing in 1% ice paraformaldehyde (PFA), the samples were analyzed using a FC 500 MCL flow cytometer (Beckman).

Multipotent differentiation

Multipotent potential of hESC-MSCs was investigated by induced differentiation toward osteogenesis, adipogenesis, and chondrogenesis as described previously [16]. Briefly, osteogenic differentiation was induced mainly by β-glycerol phosphate, dexamethasone, and ascorbic acid. Chondrogenic differentiation was induced in pellet culture with transforming growth factor (TGF)-β3 (10 ng/mL). Adipogenic differentiation was induced by treatment with 1-methyl-3-isobutylxanthine, dexamethasone, insulin, and indomethacin. Positive induction was detected by alizarin red staining, Safranin O staining, and oil red staining, respectively.

Neonatal desensitization

Neonatal rats were separated from the mother on the day of birth and received an i.p. injection of 100,000 hESC-MSCs in 1 μL sterile DMEM without serum by a handheld 10-μL SGE glass microsyringe with a 26-gauge needle. Then, they were immediately returned to their mother. After 6 weeks of birth, the rats received with or without cell injection on the

Table 1. International Cartilage Repair Society Macroscopic Evaluation of Cartilage Repair

Cartilage repair assessment ICRS	*Points*
Degree of defect repair	4
In level with surrounding cartilage	3
75% repair of defect depth	2
50% repair of defect depth	1
25% repair of defect depth	0
Integration to border zone	
Complete integration with surrounding cartilage	4
Demarcating border < 1mm	3
3/4th of graft integrated, 1/4th with a notable border < 1-mm width	2
1/2 of graft integrated with surrounding cartilage, 1/2 with a notable border < 1mm	1
From no contact to 1/4th of graft integrated with surrounding cartilage	0
Macroscopic appearance	
Intact smooth surface	4
Fibrillated surface	3
Small, scattered fissures or cracks	2
Several, small, or few, but large fissures	1
Total degeneration of grafted area	0
Overall repair assessment	
Grade I: normal	12
Grade II: nearly normal	11-8
Grade III: abnormal	7-4
Grade IV: severely abnormal	3-1

ICRS, International Cartilage Repair Society.

Table 2. Histological Scoring System for Evaluation of Overall Tissue Filling (A), Subchondral Bone Repair (B), and Cartilage Repair (C)

	Score
(A) Overall defect evaluation (throughout the entire defect depth)	
1. Percent filling with newly formed tissue	
100%	3
>50%	2
<50%	1
0%	0
2. Percent degradation of the implant	
100%	3
>50%	2
<50%	1
0%	0
(B) Subchondral bone evaluation (within the bottom 2 mm of defect)	
3. Percent filling with newly formed tissue	
100%	3
>50%	2
<50%	1
0%	0
4. Subchondral bone morphology	
Normal, trabecular bone	4
Trabecular bone, with some compact bone	3
Compact bone	2
Compact bone and fibrous tissue	1
Only fibrous tissue or no tissue	0
5. Extent of new tissue bonding with adjacent bone	
Complete on both edges	3
Complete on 1 edge	2
Partial on both edges	1
Without continuity on either edge	0
(C) Cartilage evaluation (within the upper 1 mm of defect)	
6. Morphology of newly formed surface tissue	
Exclusively articular cartilage	4
Mainly hyaline cartilage	3
Fibrocartilage (spherical morphology observed with ≥75% of cells	2
Only fibrous tissue (spherical morphology observed with <75% of cells	1
No tissue	0
7. Thickness of newly formed cartilage	
Similar to the surrounding cartilage	3
Greater than the surrounding cartilage	2
Less than the surrounding cartilage	1
No cartilage	0
8. Joint surface regularity	
Smooth, intact surface	3
Surface fissures (<25% of new surface thickness)	2
Deep fissures (≥25% of new surface thickness)	1
Complete disruption of the new surface	0
9. Chondrocyte clustering	
None at all	3
<25% chondrocyte	2
25%–100% chondrocyte	1
No chondrocytes present (no cartilage)	0
10. Chondrocyte and GAG content of new cartilage	
Normal cellularity with normal Safranin O staining	3
Normal cellularity with moderate Safranin O staining	2
Clearly less cells with poor Safranin O staining	1
Few cells with no or little Safranin O staining or no cartilage	0
11. Chondrocyte and GAG content of new cartilage	
Normal cellularity with normal Safranin O staining	3
Normal cellularity with moderate Safranin O staining	2
Clearly less cells with poor Safranin O staining	1
Few cells with no or little Safranin O staining or no cartilage	0

GAG, glycosaminoglycan.

day of birth were transplanted with the collagen bilayer scaffold seeded with or without hESC-MSCs.

Cell labeling and seeding on collagen bilayer scaffold

To detect hESC-MSCs within the site of transplantation in vivo, cells were stained with DiI (1,1-dioctadecyl-3,3,3,3-tetramethylindocarbocarbocyanine perchlorate; Invitrogen), which is stable in paraffin sections [17]. Briefly, 80% confluent cells were trypsinized and resuspended in 1.5% alginate with 10 mg/mL DiI. Ten microliters of cell suspension (5×10^7 cells/mL) was incubated with DiI for 30 min at 37°C, washed twice in phosphate-buffered saline (PBS), and seeded onto the collagen-bilayered scaffold. The hESC-MSC-seeded collagen bilayer scaffold reacted with the 102-mM $CaCl_2$ solution to form a hydrogel before transplantation.

Animal model

Adult rats (~6-week old) were anesthetized with trichloroacetaldehyde hydrate (10% m/v, 4 mL/kg), and the knee joint was opened with a medial parapatellar approach. The patella was dislocated laterally, and the surface of the femoropatellar groove was exposed. A full-thickness cylindrical cartilage defect with 2 mm in diameter and 1 mm in depth was created in the patellar groove using a stainless-steel punch. The defects were treated with the hESC-MSC-seeded bilayer collagen scaffold after neonatal desensitization (group d+s+c, $n=54$ joints), bilayer collagen scaffold alone after neonatal desensitization (group d+s, $n=16$ joints), or hESC-MSC-seeded bilayer collagen scaffold without neonatal desensitization (group s+c, $n=40$ joints). Immediately after surgery, the animals were returned to their cages without joint immobilization. A postoperative antibiotic (Gentamicin) was administered intramuscularly at 6 mg/kg per day for 3 days. After sacrifice, at least 3 knee joints from each group were collected for evaluation of inflammatory infiltration, cartilage regeneration, and hESC-MSC survival. All animals were treated according to the standard guidelines approved by the Zhejiang University Ethics Committee (No. zju2010102009).

In situ molecular imaging

To evaluate the survival of implanted cells within the cartilage defect, hESC-MSCs were stained with DiI before

transplantation, and the fluorescence signal within the implantation site was detected using a Molecular Imaging System (Carestream Health, Inc.) consisting of a CCD camera equipped with a 50-mm Nikon lens (Nikon) at the excitation wavelength of 536–560 nm.

Gross morphology and histological evaluation

Four and 8 weeks after surgery, rats were sacrificed by intravenous overdose of trichloroacetaldehyde hydrate. Joint cartilage samples from each group were examined and photographed for evaluation according to the International Cartilage Repair Society (ICRS) macroscopic assessment scale for cartilage repair (Table 1). After gross examination, samples were fixed in 4% PFA, decalcified in 4% ethylenediamine tetraacetic acid (EDTA) for 14 days, then embedded in paraffin, and cut into 7-μm sections. Sections from each sample were stained with hematoxylin and eosin (H&E) for morphological evaluation and stained with Safranin O for analysis of glycosaminoglycan distribution. A light microscope (X71; Olympus) was used for histological observation and analyzed with DP Controller 3.1.1.267 software (Olympus).

For histological scoring of the regenerated tissues within the defects, the repaired tissues were graded blindly by 3 observers, using the scoring systems established by ICRS and other researchers (Table 2) [18,19].

Biomechanical evaluation

Mechanical properties of samples 8 weeks after transplantation ($n \geq 5$ in all groups) were evaluated following the protocol reported by previous studies [20,21]. Samples were placed in PBS at room temperature for 3–4 h to equilibrate before testing. The compressive mechanical properties of the surface cartilage layer were tested with an Instron testing machine (model 5543; Instron) and software (Bluehill V2.0; Instron), using a 2-mm-diameter cylindrical indenter fitted with a 10-N maximum loading cell. The unconfined equilibrium modulus was determined by applying a step displacement (20% strain), and monitoring the compressive force over time until equilibrium was reached. The thickness of the fully relaxed cartilage layer was tested to estimate strain for applied deformations. The crosshead speed used was $\sim$0.6 mm/min. The ratio of equilibrium force to the cross-sectional area was divided by the applied strain to calculate the equilibrium modulus (in MPa).

Immunohistochemical and immunofluorescence staining

At week 1, 4, and 8 after transplantation, animals were sacrificed by trichloroacetaldehyde overdose. Knee cartilage transplanted with hESC-MSCs was cut out, decalcified, fixed, embedded in paraffin, and sectioned at 7-μm thickness. Cartilage tissues embedded in paraffin were stained for CD4 antigen (mouse anti-rat CD4 monoclonal antibody; Thermo Scientific), or human nuclear antigen (HuNu; Chemicon) according to the reported process [10] or mouse polyclonal antibodies against collagen type II (Calbiochem; Merck). Stained sections were dehydrated, mounted, inspected, and photographed using an inverted microscope (Olympus IX71).

Cell death detection

At 1 week after transplantation, knee joints in group d+s+c and group s+c were fixed, embedded in paraffin, and sectioned at 7-μm thickness. Cell death was detected by an *in situ* cell death kit (Roche). Stained sections were

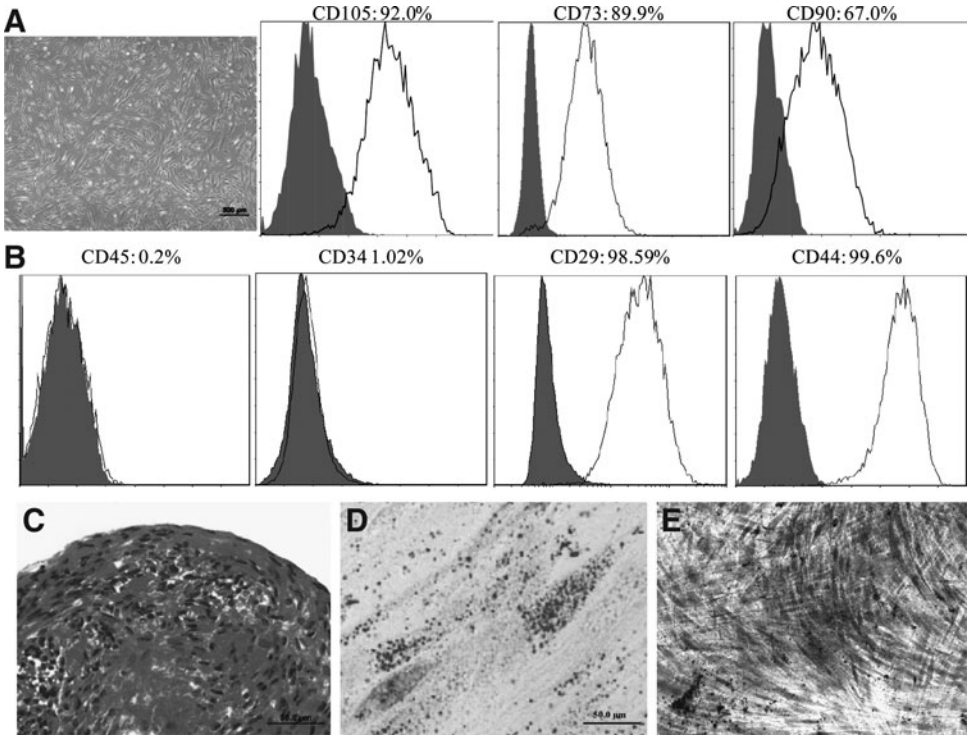

FIG. 1. Characterization of mesenchymal stem cells (MSCs) from human embryonic stem cells (hESCs). **(A)** Morphology of MSCs derived from hESCs. **(B)** Fluorescence-activated cell sorter analysis of the expression of cell surface markers in hESC-derived cells. **(C–E)** Chondrogenic, adipogenic, and osteogenic differentiation of hESC-derived cells as indicated by Safranin O staining, oil red staining, and alizarin red staining [scale bars: 500 μm in **(A)**, 50 μm in **(C, D)**, and 200 μm in **(E)**].

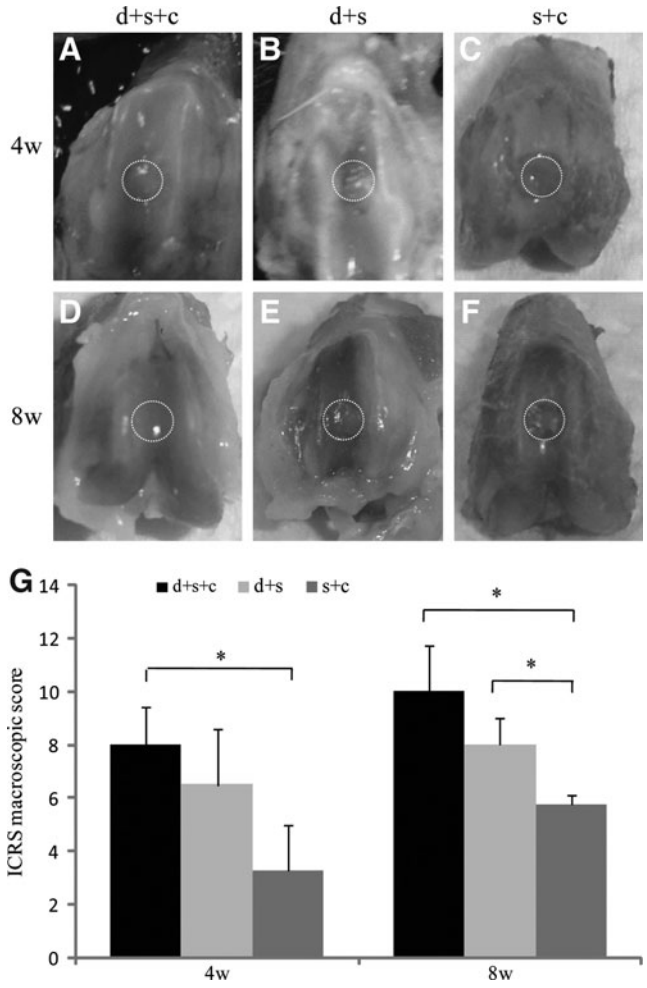

FIG. 2. Macrophotographs and ICRS scores of the defects in 3 groups 4 and 8 weeks after transplantation. Macrophotographs showed the defects in 3 groups 4 **(A–C)** and 8 **(D–F)** weeks after transplantation. **(A, D)** hESC-MSC-seeded collagen bilayer scaffold-treated group with neonatal desensitization (group d+s+c); **(B, E)** collagen bilayer scaffold-treated group with neonatal desensitization (group d+s); **(C, F)** hESC-MSC-seeded collagen bilayer scaffold-treated group without neonatal desensitization (group s+c). **(G)** International Cartilage Repair Society (ICRS) scores of groups d+s+c, d+s, and s+c 4 and 8 weeks after transplantation (maximum score=14) (*$P<0.05$ for group d+s+c vs. group vs. s+c at week 4 and 8; *$P<0.05$ for group d+s vs. group s+c at week 8). Values are represented as mean±standard deviation. *Dotted circles* indicate defects in three groups respectively.

dehydrated, mounted, inspected, and photographed using an inverted microscope (Olympus IX71).

Image quantification

To analyze the results of CD4 staining, images under high magnification were taken from each sample and quantified by ImagePro Plus (IPP) software based on the density of immunostaining. Briefly, the image was segmented first; measured by setting the threshold of density, area, and integrated optical density; and the number of CD4+ cells were automatically counted by the software. At least 5 images of different locations under high magnification from each sample were analyzed.

Statistical analysis

To assess differences in histological scoring data and biomechanical data, one-way analysis of variance with *post hoc* Student-Newman-Keuls test was used, and a P value <0.05 was considered statistically significant.

Results

hESC-derived cells exhibited MSC markers and differentiation capability of mesenchymal lineage

hESC-derived cells exhibited fibroblast-like morphology (Fig. 1A). They were CD105, CD73, CD90, CD29, and CD44 positive, but CD34 and CD45 negative (Fig. 1B). Moreover, these cells were able to differentiate into chondrocytes, adipocytes, and osteoblasts when induced with a differentiation medium in vitro (Fig. 1C–E). Collectively, these results indicate that these hESC-derived cells possess properties similar to adult MSCs, thus designated as hESC-MSCs.

Neonatal desensitization followed with hESC-MSC-seeded collagen bilayer scaffold transplantation improved cartilage regeneration

Macroscopic evaluation. Gross morphology was examined both 4 and 8 weeks after transplantation (Fig. 2). Four weeks after transplantation, group d+s+c exhibited glossy white neotissue with a flat surface and moderate integration with surrounding normal cartilage tissue (Fig. 2A). In contrast, group d+s and group s+c displayed little neotissue with an irregular surface (Fig. 2B, C). Eight weeks after transplantation, the neotissue in group d+s+c showed smooth surface and good integration with surrounding normal cartilage tissue, whereas other 2 groups still exhibited incomplete neotissue coverage (Fig. 2D–F). According to the ICRS assessment from macroscopic observations, the average scores in group d+s+c was significantly higher than groups s+c (4 weeks: 8.0±1.4 vs. 3.3±1.8; 8 weeks: 10.0±1.7 vs. 5.8±0.4; $P<0.05$); at week 8, and the average score in group d+s was also significantly higher than that in group s+c (8.0±1.0 vs. 5.8±0.4, $P<0.05$) (Fig. 2G).

Histological examination. To evaluate the cartilage regeneration, histological staining was done 4 and 8 weeks after transplantation (Figs. 3 and 4).

Four weeks after transplantation, the defect in group d+s or group s+c ($n=3$, respectively) was filled with fibrous tissue (Fig. 3B, C, E, F, H, I, K, L). In group d+s+c ($n=3$), the joint surface of the defect was repaired with a mixture of fibrous tissue and cartilage-like tissue as shown by H&E staining as well as Safranin O staining (Fig. 3A, D, G, J). In group d+s+c, the amount of chondrocyte-like cells and cartilage-like extracellular matrix was greater than group d+s and group s+c. All samples were evaluated according to the histological scoring system published before [19]. In group d+s+c, the cartilage and total scores were 5.67±2.93 and 18.5±3, respectively, with its total score significantly higher than that of group d+s (13.67±2.75) and group s+c (11.83±3.82) ($P<0.05$) (Fig. 3M, N).

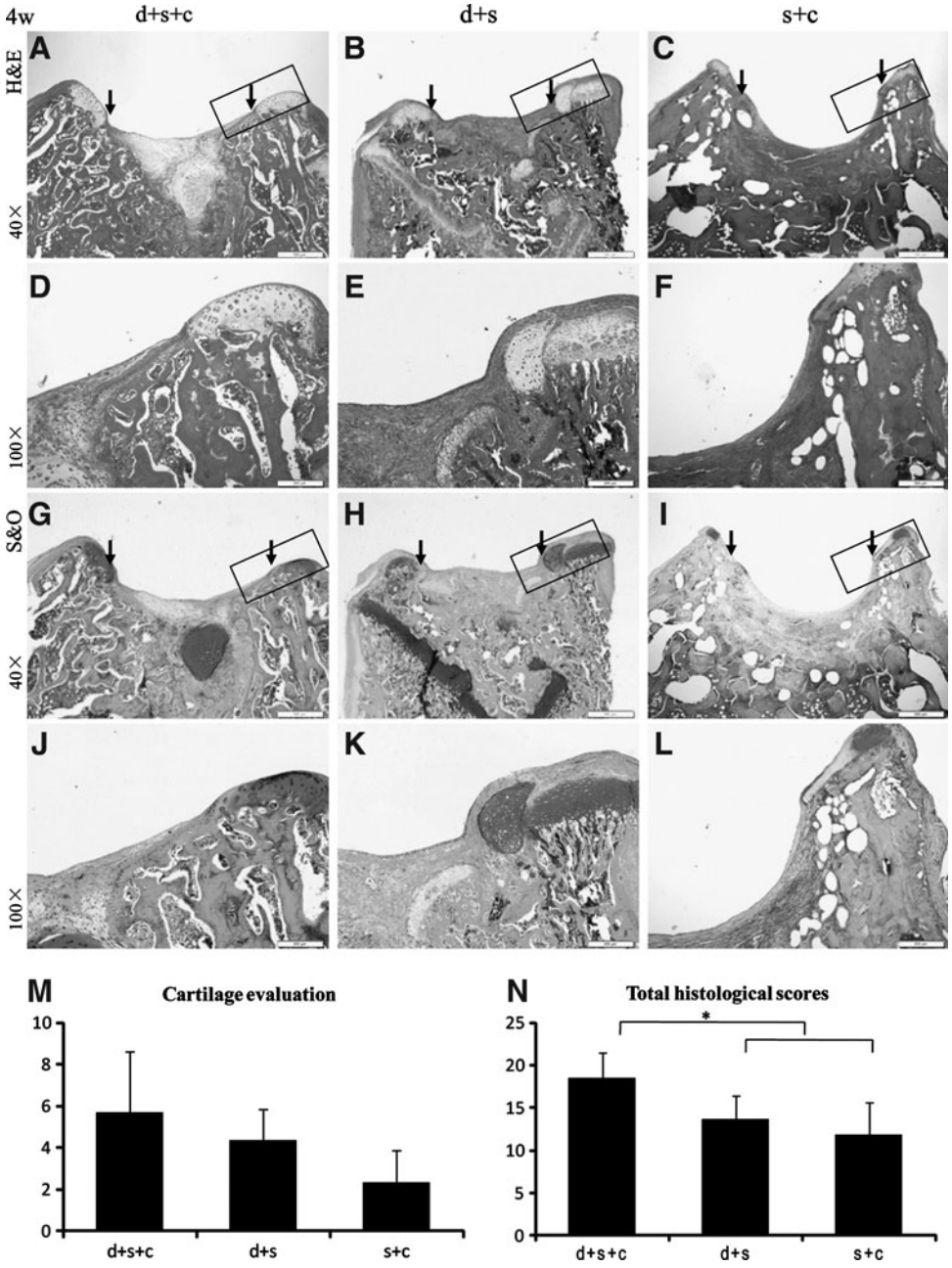

FIG. 3. Histological evaluation of 3 groups 4 weeks after transplantation with hematoxylin and eosin staining (H&E) **(A–F)**, Safranin O staining **(G–L),** and their histological scores **(M, N)**. **(A, D, G, J)** hESC-MSC-seeded collagen bilayer scaffold-treated group with neonatal desensitization (group d+s+c); **(B, E, H, K)** collagen bilayer scaffold-treated group with neonatal desensitization (group d+s); **(C, F, I, L)** hESC-MSC-seeded collagen bilayer scaffold-treated group without neonatal desensitization (group s+c); **(M, N)** Both cartilage region and total histological scores of group d+s+c (cartilage: 5.67±2.93, total: 18.5±3) were higher than those of group d+s (cartilage: 4.33±1.53, total: 13.67±2.75) and group s+c (cartilage: 2.33±1.53, total: 11.83±3.82) (*$P<0.05$ for group d+s+c vs. both group d+s and group s+c regarding the total histological score) [scale bars: 500 μm in **(A–C)** and **(G–I)**, 200 μm in **(D–F)** and **(J–L)**]. *Rectangle box* indicates the area shown in the under column with higher magnification respectively. The edge of the defect is indicated by the *black arrows*.

Eight weeks after transplantation, the defect in group d+s ($n=3$) was still filled with fibrous tissue (Fig. 4B, E, H, K), and the defect in group s+c formed bone instead of hyaline cartilage or fibrocartilage (Fig. 4C, F, I, L). Group d+s+c had the greatest amount of cartilage-like tissue, and hyaline cartilage tissues were formed at the surrounding area of the defects while fibrocartilage tissues were located at the central part of defects (Fig. 4A, D, G, J). In group d+s+c, the total score (26.63±3.86) was significantly higher than those of group d+s (20.63±2.75) and group s+c (14.50±2.00) ($P<0.05$), together with its cartilage score (10.88±3.59) significantly higher than that of group s+c (2.17±0.58) ($P<0.05$) (Fig. 4M, N).

Collagen type II immunohistochemical staining. Eight weeks after transplantation, the defect in group d+s+c filled with cartilage-like tissue was strongly positive to collagen type II antigen (Fig. 5A, D), and the repaired tissue was hard to be differentiated from the normal tissue, whereas the collagen type II-positive area was hardly detectable in group d+s and group s+c (Fig. 5B, C, E, F), and there was an obvious disconnection between the repaired tissue and the normal tissue.

Biomechanical evaluation. Young's moduli, which indicate the mechanical properties of the repaired tissue, were determined and compared 8 weeks after transplantation, and the tissue from normal rat knee joints served as normal control (Fig. 5G). At week 8, the compressive modulus of the repaired tissue in group d+s+c was around 0.056 MPa (0.056±0.008 MPa), showing significant improvement than group d+s (0.041±0.004 MPa) ($P<0.05$). However, the modulus of the repaired tissue in group d+s+c was inferior to that of normal cartilage (0.089±0.014 MPa) ($P<0.05$).

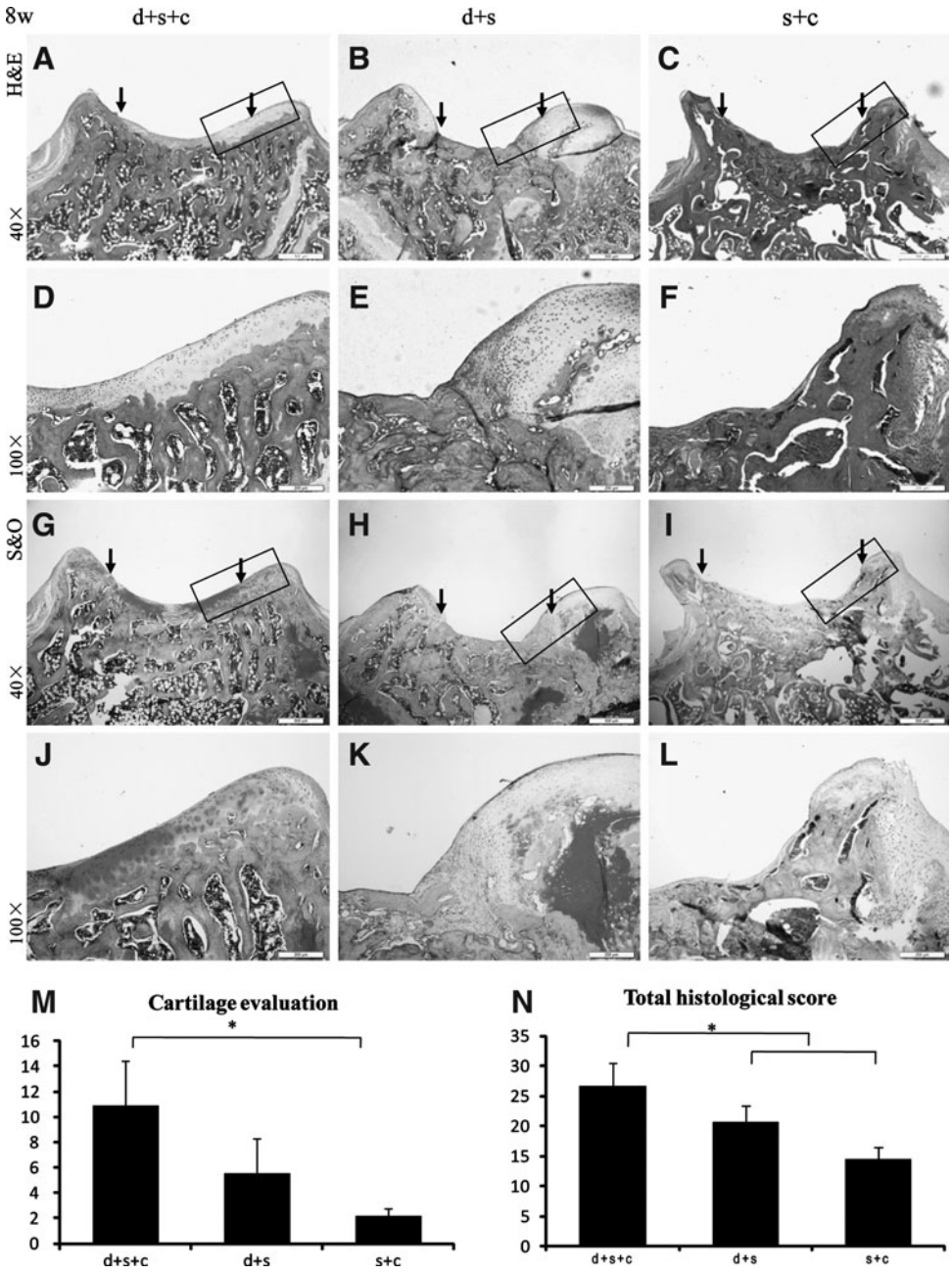

FIG. 4. Histological evaluation of 3 groups 8 weeks after transplantation with H&E staining **(A–F)**, Safranin O staining **(G–L),** and their histological scores **(M, N)**. **(A, D, G, J)** Group d+s+c; **(B, E, H, K)** group d+s; **(C, F, I, L)** group s+c; **(M, N)**. In group d+s+c, the total histological score (26.63±3.86) was significantly higher than both group d+s (20.63±2.75) and group s+c (14.50±2.00) (*$P<0.05$ for group d+s+c vs. both group d+s and group s+c). Besides that, its cartilage score was also significantly higher than group s+c (10.88±3.59 vs. 2.17±0.58, $P<0.05$) [scale bars: 500 μm in **(A–C)** and **(G–I)**, 200 μm in **(D–F)** and **(J–L)**]. *Rectangle box* indicates the area shown in the under column with higher magnification respectively. The edge of the defect is indicated by the *black arrows*.

Prolonged survival of hESC-MSCs after transplantation in desensitized rats

We also investigated the roles of neonatal desensitization on survival of hESC-MSCs after transplantation (Fig. 6). hESC-MSCs were stained with DiI and seeded onto the collagen bilayer scaffold (Fig. 6A). Image tracking showed that most of hESC-MSCs in group d+s+c were distributed at the wound site on day 10, at week 4 and 8 after transplantation (Fig. 6B, C, E), whereas no hESC-MSCs in group s+c could be found at 4 and 8 weeks after transplantation (Fig. 6D, F). Survival of hESC-MSCs in group d+s+c was further confirmed by immunofluorescence staining. Cells within the defect in group d+s+c were labeled with human nuclear antibody (Fig. 6G, H).

Reduced inflammatory cell infiltration after transplantation in desensitized rats

After we confirmed the survival of hESC-MSCs within the defect site after transplantation, we evaluated the effect of hESC-MSCs injected on the day of birth on modulating the immunoreaction of host rats to transplanted hESC-MSCs. One week after transplantation, joints from group d+s+c and group s+c were collected (Fig. 7 A, B), and tissue sections were stained for CD4. The interface area between normal and defect tissues in group s+c was positive to CD4 (Fig. 7 D, F, H), whereas there were few CD4+ T cells in group d+s+c (Fig. 7 C, E, G). Quantification of CD4+ cells by IPP software shows that the number of CD4+ cells in group d+s+c was significantly less than that in group s+c (17±5 vs. 268±107, $P<0.05$) (Fig. 7I).

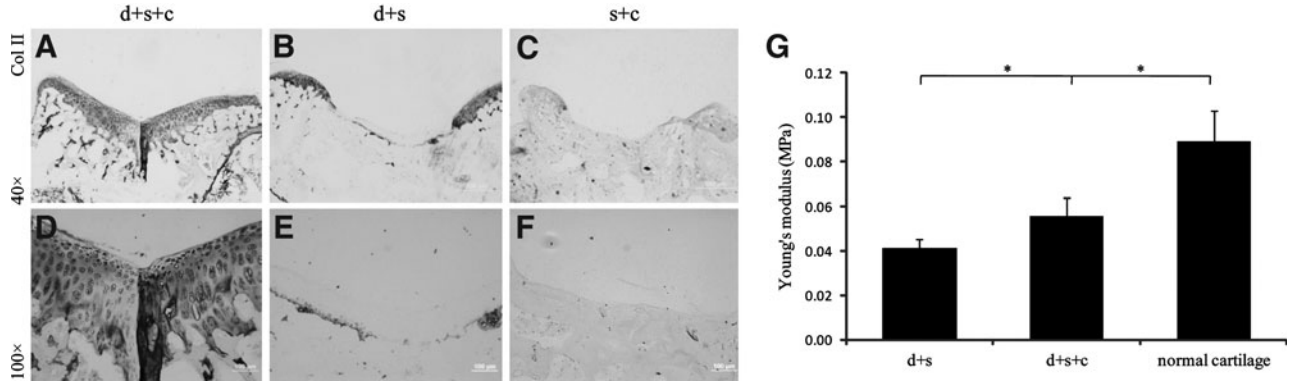

FIG. 5. Immunohistochemical staining and biomechanical evaluation of the repaired tissues 8 weeks after transplantation. Immunohistochemical staining of collagen II in the repaired tissues in group d+s+c **(A, D)**, group d+s **(B, E)**, and group s+c **(C, F)**. Abundant collagen II was exhibited in group d+s+c while hard to detect in group d+s and group s+c. **(G)** Biomechanical evaluation of the repaired tissues by mechnical test. Values were represented as mean ± standard deviation ($n \geq 5$ in all groups). The repaired tissue in group d+s+c exhibited a significantly higher compressive modulus than that in group d+s (0.056 ± 0.008 MPa vs. 0.041 ± 0.004 MPa, $^*P < 0.05$), though still lower than the normal cartilage tissue (0.056 ± 0.008 MPa vs. 0.089 ± 0.014 MPa, $^*P < 0.05$) [scale bars: 500 μm in **(A–C)**, 100 μm in **(D–F)**].

Reduced cell death after transplantation in desensitized rats

We also evaluated the effect of hESC-MSCs injected on the day of birth on acute cell death after transplantation. One week after transplantation, cell death in tissue sections from group d+s+c and group s+c was detected by an *in situ* cell death detection kit. There was little cell death detected on the cartilage surface, between the normal and the defected areas in group d+s+c (Fig. 8A, C, E), whereas abundant cell death was found in group s+c (Fig. 8B, D, F).

Discussion

ESCs can differentiate into almost all cell types and potentially provide unlimited number of cells for regenerative medicine. However, immune rejection is the major obstacle of ESC-based tissue regeneration. Induced pluripotent stem cells (iPSCs) hold a great promise for personalized regenerative medicine, because they are free of ethical issues associated with derivation of hESCs, and patient-specific iPSCs should theoretically be immune-tolerated by the recipient. However, issues such as dynamic changes in the copy numbers during reprogramming [22], epigenetic memory after differentiation [23], and tumorigenicity in vivo [24] emerged. In addition, recent studies have reported that autologous transplantation of iPSCs surprisingly induces immune rejection in recipient mice where iPSCs were derived from [25–27], questioning iPSCs as an unlimited renewable source of autologous cells without concerns of immune rejection. Thus, to the current knowledge, there is no evidence to suggest that iPSCs are superior to ESCs in terms of therapeutic application in regenerative medicine. How to use hESCs with high safety and efficacy for tissue regeneration is still an area of active research. To reduce the risk of teratoma formation, ESCs are strategically induced to differentiate into lineage-specific progenitor cells of the target tissue in a stepwise manner [28]. Our group has previously shown that hESCs could be induced to MSCs in vitro [14]. In the present study, we demonstrated that neonatal desensitization with hESC-MSCs enabled 8-week survival of hESC grafts, and hESC-MSC-seeded collagen bilayer scaffold transplantation improved the structure and function of repaired cartilage tissues.

Our results suggested that 2 factors likely contributed to the better cartilage regeneration: (1) neonatal desensitization induced immune tolerance in recipients to the xenotransplanted cells. (2) Transplanted cells were involved in tissue formation by either direct differentiation or secretion of trophic factors.

After neonatal desensitization, treatment with a construct of hESC-MSCs and collagen bilayer scaffold produced better repair as indicated by macroscopic, histological, and mechanical results at week 4 and 8. However, there was significant severe surface irregularity at the scaffold-alone group without hESC-MSCs. This immature surface would exacerbate cartilage fibrillation during scaffold degradation when cartilage lost sufficient mechanical support and was exposed to vigorous repetitive loading as indicated by previous reports [29,30]. The transplanted hESC-MSCs promoted cartilage repair possibly by direct differentiation into chondrogenic cells, which contributes directly to cartilage tissue formation, and/or secretion of trophic factors *in situ*, which promotes the subchondral bone remodeling and improves surface regularity and integration within the surrounding tissue. Our previous study has reported the secretion of growth factors such as bone morphogenetic protein (BMP)2, growth differentiation factor (GDF) 5, and FGF2 by transplanted hESC-MSCs in a tendon repair model [14]. However, in our present study, we were unable to detect the expression of *TGF-β3* and *BMPs* by RT-PCR from hESC-MSCs at 4 weeks after transplantation. This may be due to the relatively small number (500,000 cells) of transplanted hESC-MSCs. Transplantation of larger number of cells or analysis at earlier time points after transplantation would help the detection of trophic factors secreted by transplanted hESC-MSCs. Moreover, further studies with labeling hESC-MSCs before transplantation and tracing their fate after transplantation are needed to

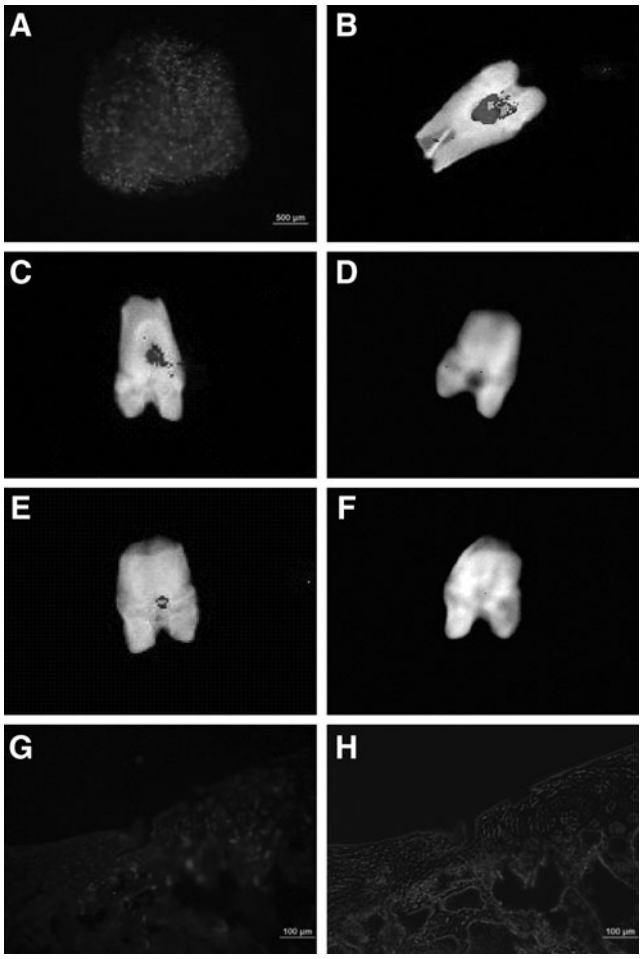

FIG. 6. Survival of hESC-MSCs within cartilage after transplantation. **(A)** hESC-MSCs were stained with DiI before transplantation; **(B)** hESC-MSCs stained with DiI were visualized by the tracking system 10 days after surgery. **(C–F)** Cooled charge-coupled device analysis demonstrated with neonatal desensitization (group d+s+c), and fluorescence signal was detected at week 4 **(C)** and 8 **(E)** after surgery, while the fluorescence signal was undetectable in group s+c **(D, F)**. **(G, H)** Immunofluorescence staining for the human nucleus in the regenerated tissues was positive in group d+s+c 4 weeks after transplantation.

evaluate the location, incorporation, and differentiation of transplanted hESC-MSCs over time in vivo, thus illustrating the full role of hESC-MSCs for cartilage regeneration.

During the preclinical study by human cell transplantation in the treatment of debilitating diseases and tissue damages, an important stage is to evaluate the survival, safety, and functional efficacy of the transplanted cells in animal models. Xenografts in the animal models are usually rejected within 2–4 weeks without appropriate immunosuppression [31]. Administration of immunosuppressant drugs such as cyclophosphamide is the mostly used approach. However, repeated macro- or microscopic testing a over long survival period is unsatisfactory. Moreover, treatments with different immunosuppressant drugs or combinations affect the survival rate and the duration of transplanted human cells [32]. Instead of immunosuppressant drug administration, long-term survival of human neural grafts in adult rats has

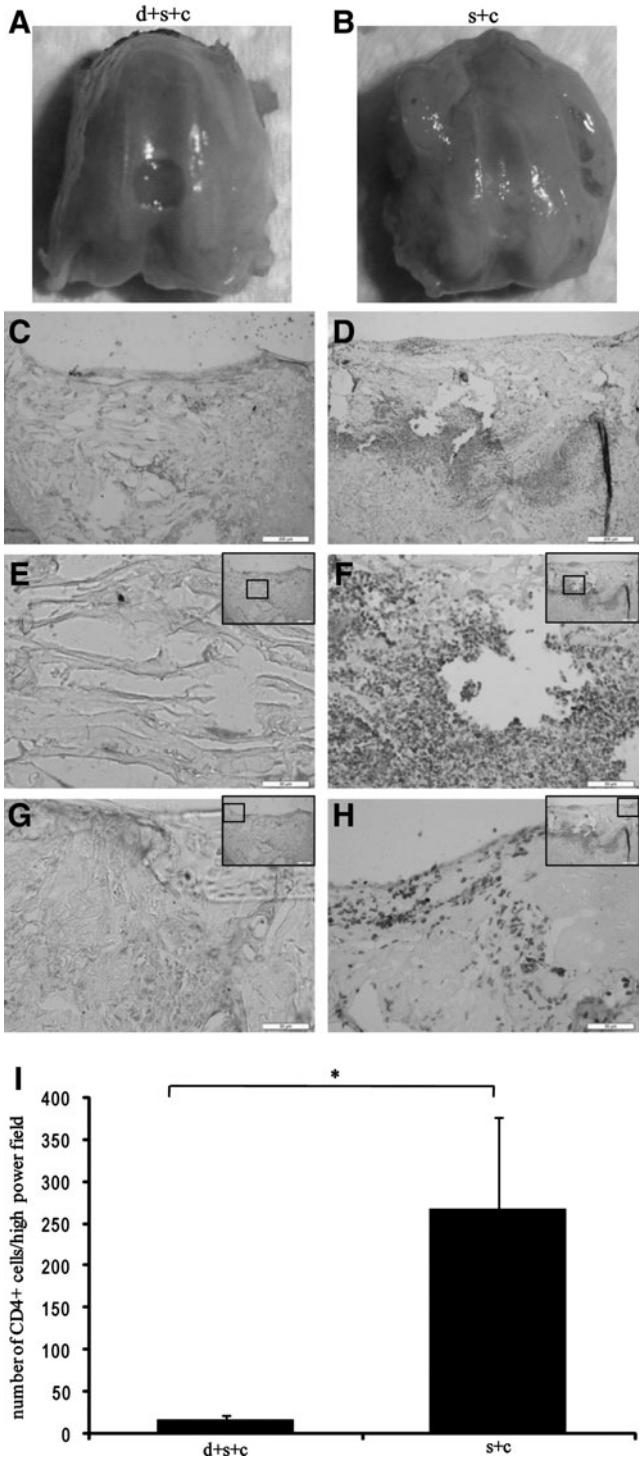

FIG. 7. Reduced inflammatory cell infiltration 1 week after transplantation in group d+s+c. Macroscopic images of the joints collected from group d+s+c **(A)** and group s+c **(B)**. **(C–H)** Inflammatory cell infiltration by CD4 staining in group d+s+c and group s+c, respectively, and its quantitative results **(I)** ($^*P < 0.05$). Images were taken from the overall view **(C, D)**, within the defect **(E, F)** and interface areas between the defect and normal tissues **(G, H)**, abundant CD4+ cells were found within the interface areas between normal and defect tissues in group s+c [scale bars: 200 μm in **(C, D)**, 50 μm in **(E–H)**]. *Insets* indicate the area and its location within the defect.

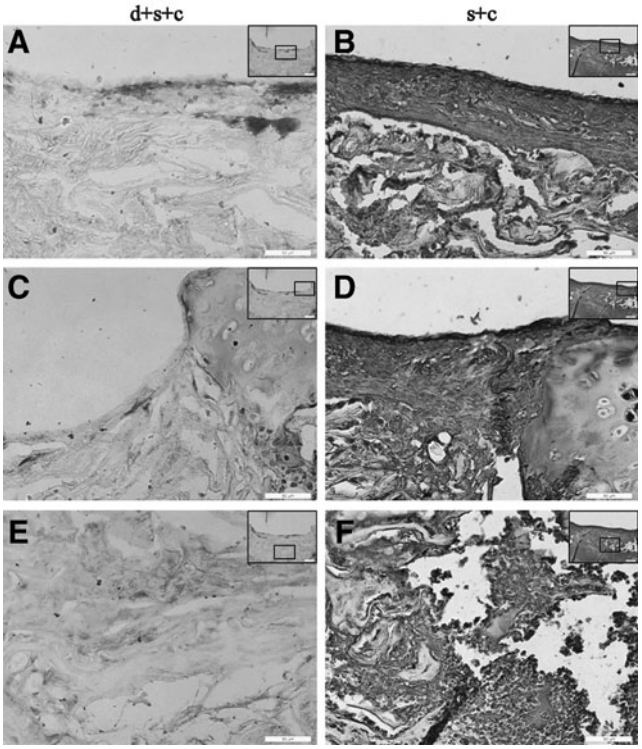

FIG. 8. Less cell death 1 week after transplantation in group d+s+c. Cell death detection by the TUNEL kit in group d+s+c **(A, C, E)** and group s+c **(B, D, F)**. Abundant cell death was found on the defect surface **(B)**, between the defect and normal tissue **(D)**, and within the defect **(F)** in group s+c (scale bars: 50 μm). *Insets* indicate the area and its location within the defect.

been achieved by desensitizing the host with neonatal injection of xenogeneic donor cells [10]. We applied this neonatal desensitization strategy in rat models for cartilage regeneration and found that xenotransplanted hESC-MSCs survived as long as 8 weeks after transplantation with neonatal desensitization pretreatment, while these xenocell grafts could not be found in other groups. Different from routine immunosuppressant drugs, neonatal desensitization did not affect the normal development of rats such as weight, eating, and drinking (data not shown). We hypothesize that injection of hESC-MSCs on the day of birth may induce immune tolerance to xenoantigens, since it is well known that new born rodents have a window to accept various foreign substances, including alloantigens [33,34], and it was proposed that the neonatal immune tolerance was not an intrinsic immune property, but was due to several mechanisms, such as T-cell anergy after interaction with epithelial cells of the host thymus [34,35], the presentation defects of immature dendritic cells [36], and increase of CD8 Treg [37]. Immune reactions were previously found in hESC-MSC-treated animals, even though the immunosuppressant was administrated, and the activity of hESC-MSCs was evaluated within 4 weeks postimplantation [14]. In this study, the finding of less CD4+ T cells in the predesensitized group (group d+s+c) 1 week after transplantation with hESC-MSC-seeded collagen bilayer scaffold supported our hypothesis. Moreover, less cell apoptosis in a predesensitized animal model would support the survival of transplanted hESC-MSCs. Prolonged survival of hESC-MSCs in a predesensitized animal model may facilitate the study of the long-term role of stem cells in human cell-based therapy in tissue regeneration, including survival, proliferation, migration, differentiation of stem cells, and their interaction with/integration to host tissue.

MSCs have been reported to be immunosuppressive. They suppressed lymphocyte activation and proliferation via soluble factors released by MSCs or direct cell–cell interaction [38,39]. However, immunogenicity of hESCs and their derivatives was yet to be studied. It was proposed that hESC-MSCs, similar to MSCs, may also have the same immunosuppressive effect, since hESC-MSCs expressed human leukocyte antigen (HLA) class I, but not HLA II molecules [40]. They reduced the proliferation of T lymphocytes responded to stimulation. Nevertheless, heavy infiltration of T cells and macrophages after xenogeneic transplantation was observed in wild-type mice [41]. One recent article reported that hESC-MSCs could ameliorate inflammatory infiltration indicated by less CD3+cell staining in a mouse model [42]. This was achieved by repeated injection, and investigation was carried out only 1 week after transplantation. Our predesensitized animal model exhibited less inflammatory infiltration indicated by less CD4+ T-cell staining, thus supporting prolonged survival of transplanted hESC-MSCs, allowing us to systematically study the immunogenicity of hESC-MSCs in vivo. Mapping out the underlying mechanism would be beneficial to the explorative study of safe and effective immunosuppressive strategies [43].

One challenge of transplanting cell suspension for tissue regeneration is to ensure reliable attachment, survival, and function of the cells within the tissue site. Polymers or matrices are adopted during transplantation as a cell delivery vehicle. Collagen has been used as an efficient cell delivery vehicle in matrix-induced ACI for cartilage repair [44]. In this study, collagen I was used to fabricate the bilayer scaffold and transplanted into the knee cartilage together with hESC-MSCs. Besides, 1.5% alginate was used to form gel upon transplantation. This may provide a microenvironment within which hESC-MSCs are protected from the immune system, survive, and participate in the regeneration process of cartilage. Inferior mechanical property of the regenerated tissue to normal cartilage was observed in our study. This may due to rapid degradation of the collagen scaffold. Collagen-based materials have shown beneficial to bone healing [45,46]; however, rapid degradation rate of pure collagen is disadvantageous [47]. Collagen scaffold could be crosslinked or combined with polymers to match the regeneration rate of tissue.

In conclusion, we presented a neonatal desensitization strategy by injection of hESC-MSCs to synergize with hESC-MSC-seeded collagen scaffold transplantation to improve the cartilage regeneration. Although it would not be possible to apply neonatal desensitization in the clinical setting, this approach eliminates the need of using immunosuppressants and avoids side effects caused by immunosuppression. It allows the assessment on the long-term fate and efficacy of transplanted hESCs and their derivatives for tissue regeneration in vivo in an immunocompetent background. This information will be instrumental in developing hESC-based therapies in the preclinical/clinical models. The possible use of this model is to extensively study the in vivo activities of

allo- or xenocell grafts, such as survival, migration, proliferation, differentiation, and functional integration, without interfering with the normal development of the animals (such as weight loss and immune system damage caused by immunosuppressants). Abundant data from such study could help to fully elucidate the role of ESCs on cell-based therapy, thus providing useful information for development of efficient preclinical/clinical models.

Acknowledgments

This work was supported by International Science & Technology Cooperation Program of China (2011DFA32190), the National Natural Science Foundation of China (81125014, J1103603, 81071461, 31000436, and 31170943), National Key Basic Research Program (2012CB966600), Zhejiang Provincial Grants (Z2100086, 2011C23079, 2012C33015), and the Fundamental Research Funds for the Central Universities.

Author Disclosure Statement

No competing financial interests exist.

References

1. Brittberg M, A Lindahl, A Nilsson, C Ohlsson, O Isaksson and L Peterson. (1994). Treatment of deep cartilage defects in the knee with autologous chondrocyte transplantation. N Engl J Med 331:889–895.
2. Kino-Oka M, Y Maeda, Y Sato, N Maruyama, Y Takezawa, AB Khoshfetrat, K Sugawara and M Taya. (2009). Morphological evaluation of chondrogenic potency in passaged cell populations. J Biosci Bioeng 107:544–551.
3. McNickle AG, DR L'Heureux, AB Yanke and BJ Cole. (2009). Outcomes of autologous chondrocyte implantation in a diverse patient population. Am J Sports Med 37:1344–1350.
4. Wakitani S, H Aoki, Y Harada, M Sonobe, Y Morita, Y Mu, N Tomita, Y Nakamura, S Takeda, TK Watanabe and A Tanigami. (2004). Embryonic stem cells form articular cartilage, not teratomas, in osteochondral defects of rat joints. Cell Transplant 13:331–336.
5. Dattena M, S Pilichi, S Rocca, L Mara, S Casu, G Masala, L Manunta, A Manunta, ES Passino, RR Pool and P Cappai. (2009). Sheep embryonic stem-like cells transplanted in full-thickness cartilage defects. J Tissue Eng Regen Med 3:175–187.
6. Fecek C, D Yao, A Kacorri, A Vasquez, S Iqbal, H Sheikh, DM Svinarich, M Perez-Cruet and GR Chaudhry. (2008). Chondrogenic derivatives of embryonic stem cells seeded into 3D polycaprolactone scaffolds generated cartilage tissue in vivo. Tissue Eng Part A 14:1403–1413.
7. Bradley JA, EM Bolton and RA Pedersen. (2002). Stem cell medicine encounters the immune system. Nat Rev Immunol 2:859–871.
8. Swijnenburg RJ, S Schrepfer, JA Govaert, F Cao, K Ransohoff, AY Sheikh, M Haddad, AJ Connolly, MM Davis, RC Robbins and JC Wu. (2008). Immunosuppressive therapy mitigates immunological rejection of human embryonic stem cell xenografts. Proc Natl Acad Sci U S A 105:12991–12996.
9. Hwang NS, S Varghese, HJ Lee, Z Zhang, Z Ye, J Bae, L Cheng and J Elisseeff. (2008). In vivo commitment and functional tissue regeneration using human embryonic stem cell-derived mesenchymal cells. Proc Natl Acad Sci U S A 105:20641–20646.
10. Kelly CM, SV Precious, C Scherf, R Penketh, NN Amso, A Battersby, ND Allen, SB Dunnett and AE Rosser. (2009). Neonatal desensitization allows long-term survival of neural xenotransplants without immunosuppression. Nat Methods 6:271–273.
11. Qi YY, X Chen, YZ Jiang, HX Cai, LL Wang, XH Song, XH Zou and HW Ouyang. (2009). Local delivery of autologous platelet in collagen matrix simulated in situ articular cartilage repair. Cell Transplant 18:1161–1169.
12. Pieper JS, A Oosterhof, PJ Dijkstra, JH Veerkamp and TH van Kuppevelt. (1999). Preparation and characterization of porous crosslinked collagenous matrices containing bioavailable chondroitin sulphate. Biomaterials 20:847–858.
13. Wang MC, GD Pins and FH Silver. (1994). Collagen fibres with improved strength for the repair of soft tissue injuries. Biomaterials 15:507–512.
14. Chen X, XH Song, Z Yin, XH Zou, LL Wang, H Hu, T Cao, M Zheng and HW Ouyang. (2009). Stepwise differentiation of human embryonic stem cells promotes tendon regeneration by secreting fetal tendon matrix and differentiation factors. Stem Cells 27:1276–1287.
15. Barberi T, LM Willis, ND Socci and L Studer. (2005). Derivation of multipotent mesenchymal precursors from human embryonic stem cells. PLoS Med 2:e161.
16. Pittenger MF, AM Mackay, SC Beck, RK Jaiswal, R Douglas, JD Mosca, MA Moorman, DW Simonetti, S Craig and DR Marshak. (1999). Multilineage potential of adult human mesenchymal stem cells. Science 284:143–147.
17. Schormann W, FJ Hammersen, M Brulport, M Hermes, A Bauer, C Rudolph, M Schug, T Lehmann, A Nussler, et al. (2008). Tracking of human cells in mice. Histochem Cell Biol 130:329–338.
18. Mainil-Varlet P, T Aigner, M Brittberg, P Bullough, A Hollander, E Hunziker, R Kandel, S Nehrer, K Pritzker, S Roberts and E Stauffer. (2003). Histological assessment of cartilage repair: a report by the Histology Endpoint Committee of the International Cartilage Repair Society (ICRS). J Bone Joint Surg Am 85-A (Suppl. 2):45–57.
19. Guo X, H Park, S Young, JD Kretlow, JJ van den Beucken, LS Baggett, Y Tabata, FK Kasper, AG Mikos and JA Jansen. (2010). Repair of osteochondral defects with biodegradable hydrogel composites encapsulating marrow mesenchymal stem cells in a rabbit model. Acta Biomater 6:39–47.
20. Chen AC, WC Bae, RM Schinagl and RL Sah. (2001). Depth- and strain-dependent mechanical and electromechanical properties of full-thickness bovine articular cartilage in confined compression. J Biomech 34:1–12.
21. Kandel RA, M Grynpas, R Pilliar, J Lee, J Wang, S Waldman, P Zalzal and M Hurtig. (2006). Repair of osteochondral defects with biphasic cartilage-calcium polyphosphate constructs in a sheep model. Biomaterials 27:4120–4131.
22. Laurent LC, I Ulitsky, I Slavin, H Tran, A Schork, R Morey, C Lynch, JV Harness, S Lee, et al. (2011). Dynamic changes in the copy number of pluripotency and cell proliferation genes in human ESCs and iPSCs during reprogramming and time in culture. Cell Stem Cell 8:106–118.
23. Kim K, A Doi, B Wen, K Ng, R Zhao, P Cahan, J Kim, MJ Aryee, H Ji, et al. (2010). Epigenetic memory in induced pluripotent stem cells. Nature 467:285–290.
24. Miura K, Y Okada, T Aoi, A Okada, K Takahashi, K Okita, M Nakagawa, M Koyanagi, K Tanabe, et al. (2009). Variation in the safety of induced pluripotent stem cell lines. Nat Biotechnol 27:743–745.

25. Zhao T, ZN Zhang, Z Rong and Y Xu. (2011). Immunogenicity of induced pluripotent stem cells. Nature 474:212–215.
26. Fairchild PJ. (2010). The challenge of immunogenicity in the quest for induced pluripotency. Nat Rev Immunol 10: 868–875.
27. Boyd AS, NP Rodrigues, KO Lui, X Fu and Y Xu. (2012). Concise review: immune recognition of induced pluripotent stem cells. Stem Cells 30:797–803.
28. Hwang NS, S Varghese and J Elisseeff. (2008). Controlled differentiation of stem cells. Adv Drug Deliv Rev 60: 199–214.
29. Shao XX, DW Hutmacher, ST Ho, JC Goh and EH Lee. (2006). Evaluation of a hybrid scaffold/cell construct in repair of high-load-bearing osteochondral defects in rabbits. Biomaterials 27:1071–1080.
30. Kerin AJ, A Coleman, MR Wisnom and MA Adams. (2003). Propagation of surface fissures in articular cartilage in response to cyclic loading in vitro. Clin Biomech (Bristol, Avon) 18:960–968.
31. Shimizu A and K Yamada. (2010). Histopathology of xenografts in pig to non-human primate discordant xenotransplantation. Clin Transplant 24 (Suppl. 22):11–15.
32. Han D, DM Berman, M Willman, P Buchwald, D Rothen, NM Kenyon and NS Kenyon. (2010). Choice of immunosuppression influences cytomegalovirus DNAemia in cynomolgus monkey (*Macaca fascicularis*) islet allograft recipients. Cell Transplant 19:1547–1561.
33. Powell TJ, Jr. and JW Streilein. (1990). Neonatal tolerance induction by class II alloantigens activates IL-4-secreting, tolerogen-responsive T cells. J Immunol 144:854–859.
34. Touraine JL and K Sanhadji. (2011). Transplantation tolerance induced in humans at the fetal or the neonatal stage. J Transplant 2011:760319.
35. Anderson G, PJ Lane and EJ Jenkinson. (2007). Generating intrathymic microenvironments to establish T-cell tolerance. Nat Rev Immunol 7:954–963.
36. Bone CA. (2005). *Neonatal Immunity*. Humana Press. New Jersey.
37. Adams B, A Dubois, S Delbauve, I Debock, F Lhomme, M Goldman and V Flamand. (2011). Expansion of regulatory CD8+ CD25+T cells after neonatal alloimmunization. Clin Exp Immunol 163:354–361.
38. Klyushnenkova E, JD Mosca, V Zernetkina, MK Majumdar, KJ Beggs, DW Simonetti, RJ Deans and KR McIntosh. (2005). T cell responses to allogeneic human mesenchymal stem cells: immunogenicity, tolerance, and suppression. J Biomed Sci 12:47–57.
39. Zappia E, S Casazza, E Pedemonte, F Benvenuto, I Bonanni, E Gerdoni, D Giunti, A Ceravolo, F Cazzanti, et al. (2005). Mesenchymal stem cells ameliorate experimental autoimmune encephalomyelitis inducing T-cell anergy. Blood 106: 1755–1761.
40. Trivedi P and P Hematti. (2008). Derivation and immunological characterization of mesenchymal stromal cells from human embryonic stem cells. Exp Hematol 36:350–359.
41. Grinnemo KH, M Kumagai-Braesch, A Mansson-Broberg, H Skottman, X Hao, A Siddiqui, A Andersson, AM Stromberg, R Lahesmaa, et al. (2006). Human embryonic stem cells are immunogenic in allogeneic and xenogeneic settings. Reprod Biomed Online 13:712–724.
42. Tan Z, ZY Su, RR Wu, B Gu, YK Liu, XL Zhao and M Zhang. (2011). Immunomodulative effects of mesenchymal stem cells derived from human embryonic stem cells in vivo and in vitro. J Zhejiang Univ Sci B 12:18–27.
43. Leveque X, E Cozzi, P Naveilhan and I Neveu. (2011). Intracerebral xenotransplantation: recent findings and perspectives for local immunosuppression. Curr Opin Organ Transplant 16:190–194.
44. Zheng MH, C Willers, L Kirilak, P Yates, J Xu, D Wood and A Shimmin. (2007). Matrix-induced autologous chondrocyte implantation (MACI): biological and histological assessment. Tissue Eng 13:737–746.
45. Rocha LB, G Goissis and MA Rossi. (2002). Biocompatibility of anionic collagen matrix as scaffold for bone healing. Biomaterials 23:449–456.
46. Akkouch A, Z Zhang and M Rouabhia. (2011). A novel collagen/hydroxyapatite/poly(lactide-co-epsilon-caprolactone) biodegradable and bioactive 3D porous scaffold for bone regeneration. J Biomed Mater Res A 96:693–704.
47. Yarlagadda PK, M Chandrasekharan and JY Shyan. (2005). Recent advances and current developments in tissue scaffolding. Biomed Mater Eng 15:159–177.

Address correspondence to:
Xiaohui Zou
Associate Professor
Clinical Research Center
The First Affiliated Hospital
School of Medicine
Zhejiang University
No. 79 Qing Chun Road
Hangzhou
Zhejiang 310003
China

E-mail: zouxiaohui@zju.edu.cn

Received for publication March 4, 2012
Accepted after revision July 12, 2012
Prepublished on Liebert Instant Online July 12, 2012